Integrated Design of Monitoring, Analysis and Maintenance for Filamentous Sludge Bulking in Wastewater Treatment

Yiqi Liu[a,b], Lingling Yuan[a], Shuo Huang[b], Daoping Huang[a], Bin Liu[*c]

[a]School of Automation Science & Engineering, South China University of Technology, Wushang Road, Guang Zhou 510640, China. (e-mail: aulyq@scut.edu.cn)

[b]Department of Systems Engineering and Engineering Management, City University of Hong Kong, Kowloon, Hong Kong. (e-mail: shuohuang7-c@my.cityu.edu.hk)

[c]Department of Management Science, University of Strathclyde, Glasgow, UK. (e-mail: b.liu@strath.ac.uk)

*Corresponding author: Bin Liu; Email: b.liu@strath.ac.uk.

Abstract: Stable operation of activated sludge process is often compromised by the occurrence of filamentous sludge bulking in wastewater treatment. Standard maintenance is implemented as a single task, which is inefficiently manipulated based on purely chemical dosage by experiences. This paper proposes a novel and efficient maintenance framework, including a set of activities: incipient fault detection, causality analysis, remaining useful life (RUL) prediction and maintenance schedule, to develop a collective strategy for sludge bulking management. In this framework, Canonical Correlation Analysis (CCA) work together with Kurtosis (KU) and an autoregressive moving average (ARMA) to identify incipient sludge bulking and to capture the evolution of sludge bulking over a long horizon. The proposed framework was tested by the collected the field data. The results showed that the proposed framework is capable of detecting (Type I error, 2.1%; Type II error, 0%), locating (root cause: temperature), calculating RUL (32-days) and maintaining sludge bulking.

Keywords: Fault diagnosis; Maintenance; Wastewater; Filamentous sludge bulking; Virtual measurement

1 Introduction

Activated sludge process (ASP) is the most commonly used technique to remove the organic material and nutrients from wastewater (Hartley, 2008; Ng, Ong, & Hossain, 2000). Successful operation of ASP highly depends on efficient biological conversions in bioreactors and normal sludge separation in secondary clarifiers. Excessive growth of filamentous bacteria in secondary clarifiers often results in sludge settleability deterioration, poor operational performance and high treatment cost (Martins, Pagilla, Heijnen, & van Loosdrecht, 2004; Olsson, 2012). This is termed as filamentous sludge bulking, which is considered as the most serious problem over 50% ASP-based Wastewater Treatment Plants (WWTPs) worldwide (Fan, et al., 2018; Guo, et al., 2013; Martins, et al., 2004; Rossetti, Tomei, Nielsen, & Tandoi, 2005). Condition-based maintenance (CBM) is a commonly used decision-making strategy to enable real-time diagnosis of incipient failure and prognosis of future system health (Allison, Dickson, Fisher, & Thrush, 2018; Kenway, et al., 2015; Bin Liu, Liang, Parlikad, Xie, & Kuo, 2017; Bin Liu, Wu, Xie, & Kuo, 2017). By resorting to condition-based maintenance, , it is desirable to transform data into knowledge to support sludge bulking management in a wastewater plant efficiently and costly (Montserrat, Bosch, Kiser, Poch, & Corominas, 2015).

Occurrence of filamentous sludge bulking mainly arises from the imbalance of bacteria in secondary clarifiers and exhibits drifting degradation pattern. Multiple sensors are usually allocated around the entire plant to gain the global insight of working status for filamentous sludge bulking, thus leading to inevitable increase of the sensory data dimensions. This high-dimension data may present redundancy and irrelevance. Statistical process monitoring, including Principal Component Analysis (PCA) (Jiang, Yan, & Huang, 2016; Merello, García-Diego, & Zarzo, 2014), Independent Component Analysis (ICA) (J.-M. Lee, Qin, & Lee, 2006) and Canonical Correlation Analysis (CCA) (Asendorf & Nadakuditi, 2017), were typically used to

refine and recognize faulty features from multisensory measurements. These methods tended to explore the data by building an empirical model. The derived model was then taken as a reference to justify the desired process behavior for the incoming data by Hotelling's T^2 or squared predicted errors (SPE). To deal with nonlinear and dynamic issues of aforementioned methods, Bayesian Networks and enhanced PCA were proposed (Baoping Cai, Liu, & Xie, 2016; B. Cai, Zhao, Liu, & Xie, 2017; Ge, 2018). If the nonlinearity with respect to a process is even complex, distributed paralleled PCA can be used by dividing such global complexity into local simplicity (Zhu, Ge, & Song, 2017). However, in the early stage of sludge bulking, the process is stationary fairly and the collected data are very limited. Linear models can provide more straightforward and more efficient ways for fault detection. Among the linear methods, CCA is able to maximize the correlation between variable groups, and identify a fault with correlated within-set covariance (Z. Chen, Ding, Zhang, Li, & Hu, 2016; Z. Chen, Zhang, Ding, Shardt, & Hu, 2016; Ding, 2014; Y. Liu, Liu, Zhao, & Xie, 2018, 2019). However, since the CCA-based process monitoring is based on correlation rather than causality among data, CCA fails to precisely locate root cause. In case of filamentous sludge bulking, it is difficult for an operator to make decisions without any information on the root cause. One of the alternatives is to resort to contribution plots (Vitale, de Noord, & Ferrer, 2015). Despite the advantages of contribution plots, it always suffers from fault smearing, i.e., the negative influence of faulty variables usually propagates to non-faulty variables. Also, contribution plots cannot suggest fault propagation graphically. In this light, integration of CCA with other methods provides potentials to deal with this issue. Root diagnosis issue has been addressed in the plant-wide oscillation identification. By performing plant-wide oscillation identification, undesired oscillations can be recognized either in the control loops or in manipulated variables (J. Lee, Kang, & Kang, 2011; Zhu, et al., 2017). Root causality diagnosis of plant-wide oscillations is mainly divided into spectral envelop, adjacency matrix, causality analysis, transfer entropy and Bayesian network (Wang, Yang, Chen, & Shah, 2016). Among these methods, Granger causality based

and transfer entropy based causality analysis are direct methods which are able to reveal variable causality using temporal data (Sarrigiannis, 2013; Vicente, Wibral, Lindner, & Pipa, 2011). However, all of the root cause analysis methods are sensitive to the noises, which is likely to cast the actual fault.

Despite the availability of fault identification methods and root cause analysis for fault detection in the early stage, rapid recovery of sludge bulking is difficult and time consuming. Accurate prediction of remaining useful life (RUL) for sludge bulking is indispensable, i.e., how much time is reserved to correct sludge bulking? The concept of RUL has been widely used in many important applications, such as product manufacturing, material science, biostatistics and econometrics. However, the critical and hidden features about RUL calculation are usually not directly observable, due to measurement delay or expensive measurement costs. Thus, increasing demand has accelerated the integration of virtual sensors (virtual measurements) to derive such hard-to-measured variables. Virtual sensors are usually used to estimate hard-to-measured (unobservable) variables by other easy-to-measured (observable) variables. To deal with the complex process behaviors, nonlinear models, such as Artificial Neural Networks (ANN), Support Vector Machine (SVM), are usually used to approach the evolutions of a quality-related but hard-to-measured variables (Zeynoddin, Bonakdari, Azari, et al., 2018). However, it is difficult to define the evolution of a variable as a purely linear or nonlinear process, but a hybrid behavior instead (Bonakdari, Moeeni, et al., 2019). Moeeni .et. al. proposed a mixture of an ARMA and an ANN model to capture such hybrid behaviors (Moeeni & Bonakdari, 2017, 2018). Another alternative is to use a purely linear model with enhanced preprocessing techniques (Bonakdari, Zaji, Binns, & Gharabaghi, 2019; Isa Ebtehaj, Bonakdari, & Gharabaghi, 2019; I. Ebtehaj, Bonakdari, Zeynoddin, Gharabaghi, & Azari, 2019). Despite their well perdition performance, the issue is that these methods are mostly limited for single-step prediction, which is not able to provide sufficient and necessary information for RUL calculation. The other important issue is that, at the onset of the evolution of sludge bulking, the collected data are always very limited

and insufficient to build nonlinear models, such as Neural Networks or Gaussian Processes Regression (H. Liu, Yang, Huang, Wang, & Yoo, 2018; Y. Liu, et al., 2019). Therefore, an ARMA (Autoregressive moving average model) model with preprocessing techniques is a better choice fairly. The ARMA-based prediction is effective with limited number of time series data being available. Also, an ARMA is able to provide models with acceptable precision and minimum parameters (Zeynoddin, Bonakdari, Ebtehaj, et al., 2018). Even though fault detection, propagation identification, causality analysis and RUL prediction have been investigated individually and intensively, few papers are devoted to jointly coordinate them for sludge bulking management. Also, none of the methodologies are qualified for the desirable features and exhibit some limitations. To address these limitations, integrating all the methods is an alternative to individual methods. Such an incorporative approach can make full use of the available information and overcome the limitations of individual methods, therefore leading to better decision making. In this work, a novel and hybrid framework for fault detection, causality analysis, fault propagation, RUL prediction and decision-making for maintenance is introduced from a systematic point of view.

Overall, condition-based maintenance cannot be seen as a single task instead, the whole aspects of maintenance must be viewed as a set of activities: fault detection, propagation identification, causality analysis, remaining useful life (RUL) prediction and maintenance strategies. Firstly, a CCA model together with Kurtosis (KU) is constructed to derive a new Squared predicted errors (SPE), SPE_{KU}, for feature extraction and fault detection. In general, CCA is able to discriminate quality-relevant and quality-irrelevant variables, and then to explore their correlation to formulate a fault detection index, i.e., SPE, for fault recognition. However, SPE index of CCA is not sensitive sufficiently for an incipient fault. In this paper, KU is utilized to refine fault-related feature with respect to SPE, in such a way that abnormal SPE signal can be amplified and captured properly. Practically, sludge volume index (SVI) is utilized to describe the sludge bulking. To justify if sludge bulking occurs, SVI values at 150

mg/L, 180 mg/L, 200 mg/L or even 280 mg/L are always documented as the control limit (Rensink, 1974). Nonetheless, even though SVI is usually used to pre-alarm sludge bulking occurrence, it is difficult to measure on-line. Moreover, due to lack of other relevant information, such as DO (Dissolved Oxygen), nutrient and so on, recognition of the root cause with respect to filamentous sludge bulking is difficult once a fault is declared by SPE_{KU}. In this light, multivariate Granger Causality (MVGC) is, secondly, proposed in this paper to assimilate more information into fault identification. By performing MVGC, the framework is able to capture the spatial and temporal dependency as well as causality among variables on one hand. On the other hand, MVGC can provide a visual cause and effect description among the variables that are most suspected to be the root cause of the sludge bulking fault in a graphical way. However, the root cause analysis will deviate significantly if improper features are forwarded into the MVGC. Thus, KU is implemented to process each raw variable before running MVGC, aiming to amplify signal variation to facilitate sequential MVGC treatment. Thirdly, an ARMA (Autoregressive moving average)-based multiple-step-ahead model serves as a virtual instrument to measure SVI over a long term. This will facilitate the relevant Remaining Useful Life (RUL) estimation and be able to achieve sufficient time for maintenance before a failure occurs. Given the resulted RUL, maintenance strategies are divided into preventive maintenance and corrective maintenance. During the preventive maintenance period, the fault evolution is not that severe. The derived root causes can be used to trigger decision-making for filamentous sludge bulking maintenance. Even though many maintenance schemes are recommended based on the output of real industries and lab research during different scenarios, few experts devote to summarization of filamentous sludge bulking maintained strategies for management. In this work, a proper preventive maintenance for many root causes is summarized. On the contrary, due to the severity of filamentous sludge bulking during the corrective maintenance period, proper chemical dosage is necessary. Because of knowledge limitation and severity of filamentous sludge bulking, the majority of operators prefer to dose chemicals directly,

which implies improper cost saving and insufficient time saving for maintenance. Overall, to ensure that filamentous sludge bulking can be managed in a timely and cost-effective way, this paper classifies the entire maintenance period into preventive and corrective maintenance. As a first attempt, preventive maintenance is mainly used to deal with incipient sludge bulking, such as adjustment of operational parameters. Once the preventive maintenance strategy does not work well, corrective maintenance has to be triggered, which is to dose chemicals up to the seriousness.

Section 2 presents the novel framework for the condition-based maintenance of sludge bulking. The proposed methodologies are validated and discussed using simulation with operational data being collected from a full-scale wastewater treatment plant (WWTP) in Section 3. Conclusions are drawn in Section 4.

2 The Proposed Framework

The proposed framework is shown in Fig. 1 and defined as following:

(1) Fault detection: selected variables and samples are fed to train and test a CCA model. The SPE derived from the CCA model is then treated by the KU. Once an incipient fault is recognized by SPE_{KU}, the procedure will step into fault location at the stage (2) and RUL prediction at the stage (3). That is to say, root cause analysis and RUL calculation will be triggered once an incipient sludge bulking is recognized. Otherwise, it will go back to fault detection if a new sample arrives. (2) Fault location: once an incipient fault is declared, KU is used to refine more sensitive features from selected variables to justify if significant change is happening. The extracted features are re-organized with the variation sequence against the time. That is to say, the variable with the earliest jump could be most potential rooting cause and will be picked up to be the highest priority in the feature matrix. The derived feature matrix will be then fed to MVGC for root cause analysis. (3) RUL prediction: once the predicted SVI crosses over the SPE_{KU} control limit, the RUL will be calculated based on the multi-step prediction of an ARMA model. The ARMA model will make multi-step prediction of SVI until the predicted SVI values reach the control limit,

200mg/L. (4) Maintenance: based on the derived RUL and the profile of a fault propagation given by the MVGC, maintenance decisions can be suggested relying on the summarized expert knowledge. Preventive maintenance, such as adjustment of operational parameters, is used to deal with incipient sludge bulking. Once the SVI attains corrective control limit (CCL_{limit}), corrective maintenance has to be triggered, which is to dose chemicals up to the seriousness.

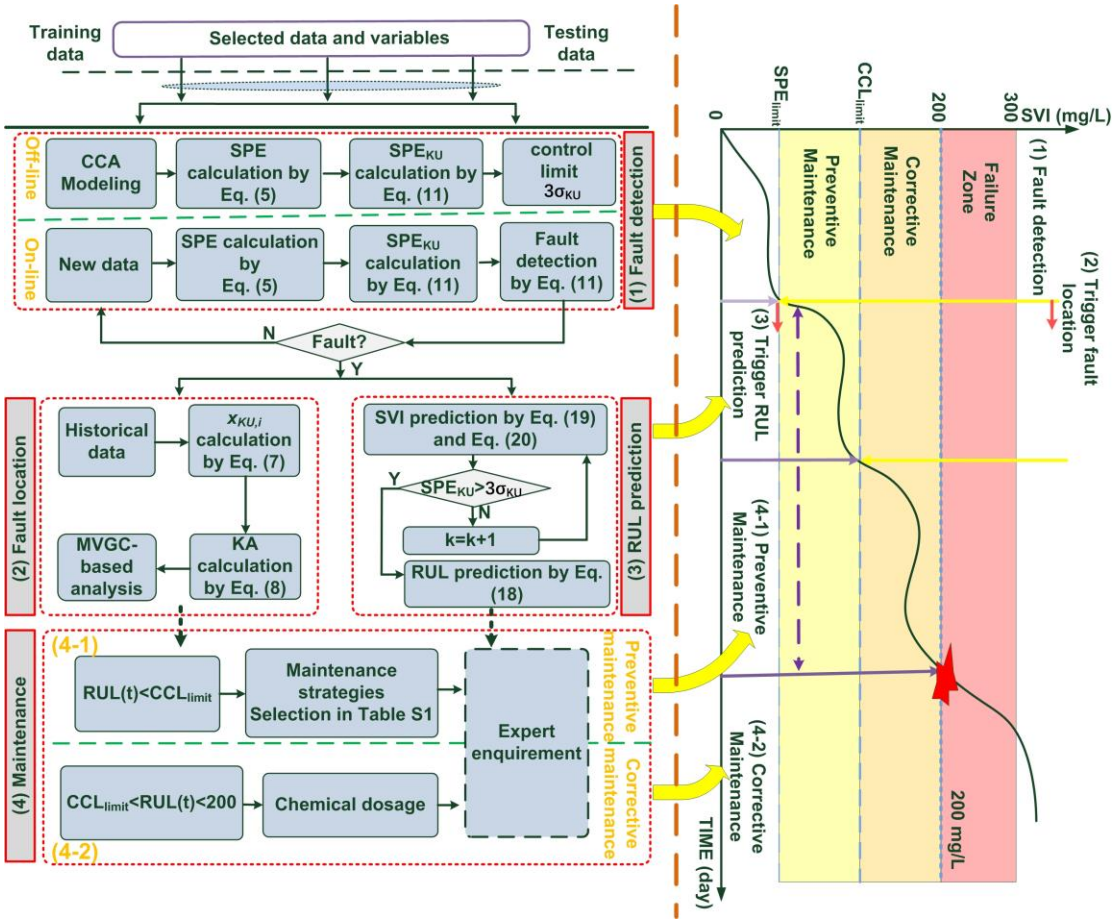

Fig. 1 Schematic diagram of algorithm implementation

2.1 CCA-based fault identification

CCA is a method to correlate two vectors by maximizing correlations among them. Suppose that N samples of the process data are collected, and X_1 and X_2 represent input variables and response variables, respectively, where $X_1 \in \mathbb{R}^{d_1 \times N}$ and $X_2 \in \mathbb{R}^{d_2 \times N}$, $d = d_1 + d_2$. d_1 and d_2 represent the number of variables for X_1 and X_2, respectively. Let X_1 and X_2 be centered by mean, then

$$\begin{bmatrix} \Sigma_{X_1X_1} & \Sigma_{X_1X_2} \\ \Sigma_{X_2X_1} & \Sigma_{X_2X_2} \end{bmatrix} \approx \frac{1}{N} \begin{bmatrix} X_1{X_1}^T & X_1{X_2}^T \\ X_2{X_1}^T & X_2{X_2}^T \end{bmatrix} \quad (1)$$

Let the matrix Σ_{T}

$$\Sigma_{\mathrm{T}} = \Sigma_{\mathrm{X_1X_1}}^{-1/2}\Sigma_{\mathrm{X_1X_2}}\Sigma_{\mathrm{X_2X_2}}^{-1/2} \quad (2)$$

By performing the singular value decomposition (SVD) on the matrix,

$$\Sigma_{\mathrm{T}} = \mathrm{U}\Lambda\mathrm{V}^{\mathrm{T}} \quad (3)$$

Two canonical correlation vectors with respect to X_1 and X_2 can be defined as $J = \Sigma_{X_1X_1}^{-1/2}U(:,1:l)$ and $L = \Sigma_{X_2X_2}^{-1/2}V(:,1:l)$, where l is the number of selected components and $l \leq min\ (d_1, d_2)$. The residual vectors are defined for as follows,

$$e = \mathrm{L}^{\mathrm{T}}X_2 - \Lambda_l J^{\mathrm{T}}X_1 \quad (4)$$

Squared predicted errors (SPE) can be formulated as follows:

$$SPE = e^T e \quad (5)$$

The derived SPE is then taken as a reference to justify the desired process behavior for the incoming data. In order to recognize the dissimilar behaviors properly, the control limit is defined necessarily as follow:

$$SPE_{\mathrm{lim}} = \varsigma\chi_{1-\alpha}^2(\tau) \quad (6)$$

where $\varsigma = \Sigma_{SPE}/2\mu_{SPE}$, $\tau = 2\mu_{SPE}^2/\Sigma_{SPE}$, Σ_{SPE} and μ_{SPE} are estimated mean and variance of R, α is the significance level and can be defined as 99%, 95% and 90%, generally. Typically, CCA is able to act as process monitoring model. However, since CCA is not sensitive to incipient fault, fault feature is usually missed.

2.2 Kurtosis-based Feature extraction

Kurtosis is one of the typical and efficient ways being able to capture signal variations. The reason why Kurtosis indicator works well for feature extraction is that it is able to measure the heaviness of the tails in the distribution of signal, thus leading to high values of the kurtosis parameter. Therefore, the kurtosis could be used to identify changes in signals. Kurtosis value is on where $x_i(t)$, $i = 1,2,\cdots,d$ and $t = 1,2,\cdots,N_t,\cdots,N$, is the time series signal taken from X_1 or X_2. d is the number of variables and N is the number of sampling points. As shown in Eq. (7), σ_i^4 in denominator is able to amplify the unstable variations and further extract the faulty features (de la Rosa, Agüera Pérez, Palomares Salas, & Sierra Fernández, 2015;

Joanes & Gill, 1998).

$$KU_i = \frac{\sum_{t=1}^{N_t}(x_i(t)-\bar{x}_i)^4}{(N_t-1)\sigma_i^4} \quad (7)$$

KU_i represents the KU value with respect to the *i*th variable, whereas $\mathrm{KU}_i(t)$ represents the KU value with respect to the *i*th variable at the sample time, *t*. To identify the variation, we also define the amplitude as follows:

$$KA_i = \frac{\mathrm{KU}_i(t)-\mathrm{KU}_i(t-m)}{\mathrm{KU}_i(t)} \quad (8)$$

where m is the number of delay steps and can be determined by auto-correlation analysis and partial-correlation analysis. The purpose of Eq. (8) is to ensure that change points of KU_i can be identified timely. $\bar{x}_i$ is the mean value of the signal x_i in the interval of [1, N_t] is defined as

$$\bar{x}_i = \frac{1}{N_t}\sum_{t=1}^{N_t} x_i(t) \quad (9)$$

σ is the standard deviation of the signal and is given as

$$\sigma_i = \sqrt{\frac{1}{N_t-1}\sum_{t=1}^{N_t}(x_i(t)-\bar{x}_i)^2} \quad (10)$$

Due to the normalization, *KU* values are assumed to follow Gaussian distributions. Also, let $x_i(t) = SPE_i(t)$ and substitute $x_i(t)$ into Eq. (7), the $\mathrm{SPE}_{\mathrm{KU}}$ can be derived as Eq. (11) and justified by 3-sigma limits (three times standard deviations) can serve for fault detection.

$$\mathrm{SPE}_{\mathrm{KU},i}(\mathrm{t}) = \left|\frac{\mathrm{KU_i(t)}-\overline{\mathrm{KU_i}}}{\sigma_{\mathrm{KU}}}\right| \le 3\sigma_{\mathrm{KU}} \quad (11)$$

where $\overline{\mathrm{KU_i}}$ and σ_{KU} represent the mean values and standard variance of KU_i. Once $\mathrm{SPE_{KU}(t)}$ value at the sample time *t*, i.e., $\mathrm{SPE_{KU}(t)}$, crosses over the control limit $3\sigma_{\mathrm{KU}}$, a fault state will be declared. Otherwise, it will not.

In this paper, KU is used for two folds. One is for feature extraction of SPE to enhance fault detection as aforementioned in the stage (1): Fault detection. Generally, CCA-based fault detection is insensitive to incipient faults. Kurtosis is able to make SPE more sensitive to incipient faults as shown in Eq. (11). The other function of Kurtosis is to refine the features from original variables and then feed to MVGC, aiming to provide preliminary sequence information for MVGC. Depending on the assumption that the variable with the earliest and significant variations could have

more potential to be the rooting cause, movement of the variable with the earliest and significant variations to lower dimension of the input matrix is able to facilitate MVGC analysis. This is mainly due to the fact that MVGC is based on the time series analysis and is heavily temporal correlation. Thus, the feature feeding to MVGC can be defined similarly as Eq. (7).

2.3 MVGC-based root cause analysis

Since CCA-based process monitoring is based on correlation rather than causality among data, CCA technology cannot locate exact rooting cause. In case an abnormality occurs in an industrial process, it is difficult for an operator to take accurate actions to diagnose the root cause of a fault. Also, due to the closed-loop structure of an OD process, the sludge bulking fault is not limited in a local unit, but rather propagates as global variations. This phenomenon is featured by causality which can approach the cause-effect relationship among different variables. Reorganization of the causality is to find the root cause and present the fault propagation paths before maintenance. Granger causality test is one of the approaches to deal with this issue. The main motive behind the Granger causality test is to identify causality by determining if one time series is useful in forecasting another. Also, Granger causality test is a graphical model and can provide an intuitive way to present causality.

Assuming that x_1 and x_2 are two time-series variables selecting from X_1 or X_2. A time series x_1 is said to Granger-cause x_2 if x_1 values provide statistically significant information about future values of x_2 through a series of *t*-tests and *F*-tests. Suppose that the temporal dynamics of two time series $x_1(t)$ and $x_2(t)$ with time lag being length *p*

$$I(t) = \begin{pmatrix} x_1(t) \\ x_2(t) \end{pmatrix} \tag{12}$$

To qualify the G-causality from $x_2(t)$ to $x_1(t)$, $F_{2\to1}$ is used to stands for the "degree to which the past of $x_2(t)$ helps predict $x_1(t)$, over and above the degree to which $x_1(t)$ is already predicted by its own past". To approach causality, a VAR (Vector Auto-regressive) model is always used. In the VAR model, the VAR(*p*)

decomposes as

$$\begin{pmatrix} x_1(t) \\ x_2(t) \end{pmatrix} = \sum_{j=1}^{p} \begin{pmatrix} A_{11,j} & A_{12,j} \\ A_{21,j} & A_{22,j} \end{pmatrix} \begin{pmatrix} x_1(t-j) \\ x_2(t-j) \end{pmatrix} + \begin{pmatrix} \varepsilon_1(t) \\ \varepsilon_2(t) \end{pmatrix} \quad (13)$$

where p is the maximum number of lagged observations or the model order, A represents the coefficients of the model, and ε_1, ε_2 are the residuals (prediction errors) for each time series. The residuals covariance is given as

$$\Sigma = cov\begin{pmatrix} \varepsilon_1(t) \\ \varepsilon_2(t) \end{pmatrix} = \begin{pmatrix} \Sigma_{11} & \Sigma_{12} \\ \Sigma_{21} & \Sigma_{22} \end{pmatrix} \quad (14)$$

The regression with respect to $x_1(t)$ is defined as follows:

$$x_1(t) = \sum_{j=1}^{p} A_{11,j} x_1(t-j) + \sum_{j=1}^{p} A_{12,j} x_2(t-j) + \varepsilon_1(t) \quad (15)$$

By exclusion of effect induced by $x_2(t)$

$$x_1(t) = \sum_{j=1}^{p} A_{11,j} x_1(t-j) + \varepsilon_1^{'}(t) \quad (16)$$

Defining $cov(\varepsilon_1) = \Sigma_{11}$ and $cov(\varepsilon_1^{'}) = \Sigma_{11}^{'}$. Thus the G-causality from $x_2(t)$ to $x_1(t)$ is defined to be the log-likelihood ratio

$$\mathrm{F}_{2\to 1} = ln\frac{|\Sigma_{11}^{'}|}{|\Sigma_{11}|} \quad (17)$$

G-causality in Eq. (17) can quantify the reduction in prediction error when the past of the process $x_2(t)$ is included in the explanatory variables of a VAR model for $x_1(t)$. If the variance of ε_1 is reduced by the inclusion of x_2 in the Eq. (16), then it is said that x_2 G-causes x_1. Also, G-causality is easy to generalize to the multivariate (conditional) case in which the G-causality of $x_2(t)$ on $x_1(t)$ is tested in the context of multiple additional variables $x_3(t), \cdots, x_d(t)$. More details can be found in the MVGC toolbox (Seth, 2010).

2.4 RUL prediction

The purpose of prognosis is to predict the time to failure of a degrading component or subsystem, also called remaining useful life (RUL), by assessing the current degradation state of a component or subsystem, its past degradation trend or profile given by the continuous monitoring module with the known future operating conditions of the component or subsystem. RUL is the time left before a component or subsystem, which is assigned for a particular job or a function, reaches its end of life. In the ASP process, SVI is always chosen to indicate the evolution of the sludge

bulking, thus SVI is selected as an evaluation variable to calculate RUL. RUL of sludge bulking can be expressed as

$$RUL = \inf\{t: x_{SVI}(t) \geq C | x_{SVI}(0) < C\} = t_f - t_0 | t_f > t_0 \quad (18)$$

where t_f signifies the random failure time, t_0 signifies the current age. C is the threshold level and x_{SVI} is the SVI variable. To predict *RUL*, the evolution variable, SVI, is obtained necessarily. Degrade However, SVI cannot be observed directly. ARMA model serve as a virtual instrument to predict SVI over a long period in this paper. During the long-term prediction, historical and currently measured values are collected and served as the starting point for the first step prediction. Then, the multi-step ahead prediction based on an ARMA model is performed in a subsequent iterative way. Based on the ARMA model obtained through the above steps, iterative multi-step prediction is provided in as follows, where *k* is the steps of prediction:

When $1 < k \leq n_c$,

$$\hat{x}_{SVI}(t_0 + k|t_0) = \sum_{i=1}^{n_a} a_i \hat{x}_{SVI}(t_0 + k - i|t_0) + \sum_{i=k}^{n_c} c_i \hat{v}(t_0 + k - i) \quad (19)$$

where $\hat{x}_{SVI}$ are the predicted values of SVI and $\hat{v}(t), \hat{v}(t-1), \cdots, \hat{v}(t+k-n_c)$ can be estimated by the Recursive Extended Least Square (RELS) method. More details can see the reference (J. Chen, Ganigue, Liu, & Yuan, 2014). n_a, n_c are the orders of a and c ,respectively.

When $k > n_c$,

$$\hat{x}_{SVI}(t_0 + k|t_0) = \sum_{i=1}^{n_a} a_i \hat{x}_{SVI}(t_0 + k - i|t_0) \quad (20)$$

when $t_0 + k - i \leq t_0$, $\hat{x}_{SVI}(t_0 + k - i|t_0) = x(t_0 + k - i)$. Therefore, assuming the prediction horizon $L > n_c$, multi-step optimal prediction $\hat{x}_{SVI}(t_0 + k|t_0)$, $k = 1,2, \cdots h_1$ can be recursively obtained by applying the estimated values $\hat{a}_i$, $\hat{c}_i$, $\hat{v}(t_0), \cdots, \hat{v}(t_0 + k - n_c)$ to replace a_i, c_i, $v(t), \cdots, v(t_0 + k - n_c)$ in Eq.(19) and Eq.(20). h_1 is the terminal point during the prediction horizon.

2.5 Maintenance

The challenge afterward mainly lies in decision-making after identifying the root cause of sludge bulking. Even though many schemes have been proposed to deal with this problem, few experts devote to summarize this field knowledge.

Table 1 Causal matrix for filamentous sludge bulking

Monitored variables and their abbreviation	**T**	**BOD_5**	**TP**	**COD**	**SNO**	**SRT**	**MLSS**	**TN**	**SVI**
(1) Temperature (T)	NaN	0.0075	0.0003	0.0076	0.0005	0.0126	0.0089	0.0013	0.0265
(2) Biological Oxygen Demand concentration in effluent for five days (BOD_5)	0.0135	NaN	0.0447	0.0032	0.0001	0.0001	0	0	0.0010
(3) Total phosphorus (TP)	0.0008	0.0172	NaN	0.0001	0.0001	0.0001	0.0085	0.0023	0.0111
(4) Chemical Oxygen Demand (COD)	0.1099	0.0199	0.0091	NaN	0.0138	0.0159	0.0080	0.0178	0.0074
(5) NO_2-N (SNO)	0.0357	0.0094	0.0347	0.0046	NaN	0.0007	0.0076	0.0129	0.0007
(6) Sludge Retention Time (SRT)	0.0024	0.0028	0.0002	0.0038	0	NaN	0.0112	0.0408	0.0380
(7) Mixed liquid suspended solids (MLSS)	0.0236	0.0291	0.0444	0	0.0071	0.0331	NaN	0.0190	0.0131
(8) Total nitrogen concentration in effluent (TN)	0.0091	0.0068	0.0589	0.0315	0.0167	0.0010	0.0293	NaN	0.0089
(9) Sludge Volume Index (SVI)	0.2748	0.0092	0.0002	0.0001	0.0351	0.0009	0.1181	0.008	NaN

(1), … , (9) REPRESENT THE ORDER OF VARIABLES IN THE MVGC ANALYSIS; (X1) MEANS THIS VARIABLE IS IN THE VECTOR X1; (X2) MEANS THIS VARIABLE IS IN THE VECTOR X2;

As profiled in Fig.1, deterioration of sludge bulking typically becomes more severe as the time evolution. For different stage, we have to take different actions. Firstly, we summarized the basic preventive maintenance strategies from many WWTPs as Table S1. Preventive maintenance is performed as Table S1 (Supplementary Information), once Eq. (10) is met (SPE_{KU} control limit). Also, RUL can be derived by calculating Eq. (18) in this stage. By investigating Table S1 deeply, nine typical Sludge bulking scenarios are summarized with respect to different root cause.

For some cases, preventive maintenance is not able to approach sludge bulking completely. To ensure sufficient time to perform the corrective maintenance if crossing over the corrective control limit, we define the corrective control limit (CCL_{limit}) as follows:

$$\hat{x}_{SVI} > 50\%(200 - \mathrm{SPE}_{\mathrm{KU}}) = CCL_{limit} \quad (21)$$

50% was derived by trading off the volume of dosed chemicals, the type of dosed chemicals as well the severity degree of sludge bulking by the field experts. During the corrective maintenance, we have to further added coagulants or $FeSO_4$ to kill filamentous bacteria. However, once SVI cross over 200 mg/L, we have to shut down the wastewater plant to avoid polluted wastewater discharge into river.

3 Results and discussions

The proposed predictive CBM framework is assessed by a full-scale Oxidation Ditch (OD) WWTP in Beijing. This section describes the detail of the corresponding WWTP with filamentous sludge bulking.

3.1 A full-scale WWTP with an OD treatment

In this case study, a full-scale WWTP (Beijing, China) with a modified activated sludge process is presented for assessment (Fig. 2). This modified treatment process is able to improve biodegradable organics removal by resorting to utilize long solids retention times (SRTs). The main parameters of this WWTP are shown as follows: the average influent flow is about 170, 000 m^3/d; an average OD hydraulic retention time (HRT) is 16.5 h; SRT is equal to 15-22 d. The main reason why OD is applied in many WWTPs is that removal performance can be achieved with lower weir overflow rate, less sludge production and more energy savings. However, due to the larger land area requirement than typical activated sludge treatment processes, suspended solids concentrations in the discharge of a WWTP occurs frequently. Filamentous sludge bulking occurred due to the significant temperature decrease in this case. All data are sampled at one-day interval. The selected monitored variables for model construction are shown as Table S2 (Supplementary Information). 213 data points are sampled from the field at day interval. From the 70^{th} day of the collected data, filamentous sludge bulking has occurred slightly due to the low temperature of influent and lasts over about half a year. During this period, part of polluted wastewater has been flowed into the river without any declaration.

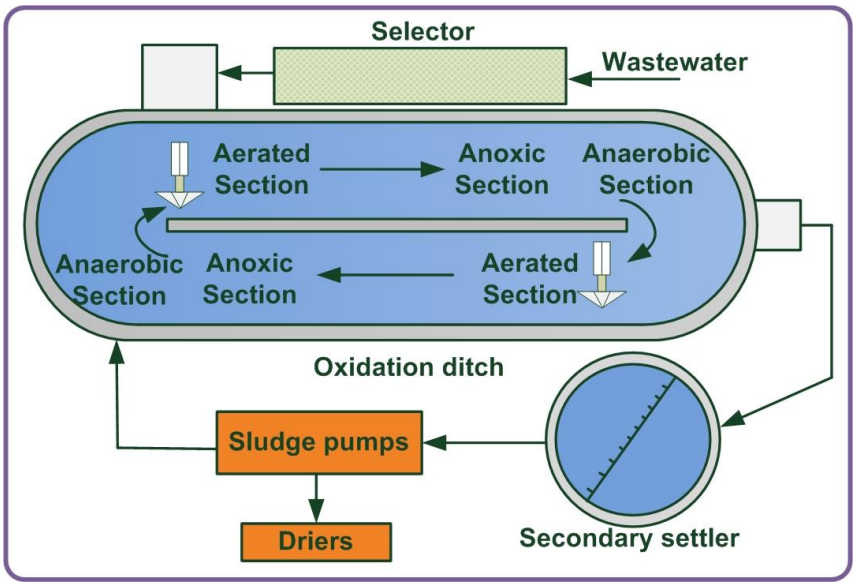

Fig. 2 Schematic diagram of a full-scale oxidation ditch process

The reason why filamentous sludge bulking is difficult to control mainly lies on the fact that, based on evidence provided by microbiological observations by Ovez and Orhan (Ovez S, 2007), chemical dosage for most cases provides only temporary and superficial way for the treatment of filamentous sludge bulking. The existence of uncertainties, such as weather, operation, and so on, adds further complexity for filamentous sludge bulking. Therefore, it is imperative to propose a framework to support filamentous sludge bulking, which can also be assisted with the expert knowledge.

3.2 Performance evaluation criteria

To evaluate the performance of CCA-based fault detection, both of Type-I error (faulty detection rate) and Type II error (false alarm rate) are used in this paper (Narayana Moorthy, Martins, Sousa, Ramos, & Fernandes, 2014). Type-I error is to describe how many faulty samples are mis-identified as normal samples. Thus, $\text{Type I error} = \frac{\text{number of mis-identified faulty samples}}{\text{total number of faulty samples}}$. On the contrary, Type-II error is to describe how many normal samples are mis-identified as faulty samples. Thus, $\text{Type II error} = \frac{\text{number of mis-identified normal samples}}{\text{total number of normal samples}}$.

The Root Mean Square Error (RMSE) and correlation coefficient (r_c) were used to assess the prediction performance of ARMA model. The RMSE is defined as follows for quality comparisons of different models:

$$RMSE = \sqrt{\frac{1}{N}\sum_{i=1}^{N}(y_i - \hat{y}_i)^2} \tag{23}$$

where y_i and $\hat{y}_i$ are the measured and prediction values, respectively. The correlation coefficient (r_c) is quantified as follows:

$$r_c = \frac{\sum_{i=1}^{N}(y_i - y_i')(\hat{y}_i - \hat{y}_i')}{\sqrt{\frac{1}{N}\sum_{i=1}^{N}(y_i - y_i')^2}\sqrt{\frac{1}{N}\sum_{i=1}^{N}(\hat{y}_i - \hat{y}_i')^2}} \tag{24}$$

y_i' and $\hat{y}_i'$ are the mean of y_i and $\hat{y}_i$, respectively. N is the number of datasets.

3.3 Fault detection

The purpose of this section is to detect an incipient fault as early as possible, which will facilitate the fault pre-caution and guarantee sufficient time for sequential maintenance. In our methods, CCA is used for incipient fault detection firstly. The number of latent variables for CCA, l, is selected as 5. $X_1 = [SRT, T, MLSS, SNO, COD]$ and $X_2 = [TP, BOD_5, TN, SVI]$. X_1 is a vector consisting of easy-to-measured variables, whereas X_2 is composed of the hard-to-measured variables in the discharge of the wastewater plant. For the 213 data points, 50 samples are used for fault detection model training, whereas the remaining is used for testing. By performing Eq. (4)-(6), it is obvious in Fig. 3 (a) that the SPE is able to detect the fault until the 120th day of the testing set approximately. To achieve better performance of fault detection in our methodology, KU is further used to enhance the SPE signals of CCA to refine the fault features. On the basis of Eq. (11), SPE_{KU} and its control limit are derived. Due to the incorporation of KU, the SPE_{KU} is able to recognize the incipient fault at the 23rd day of testing set, which is 97 days earlier compared with the pure SPE index of CCA (Fig. 3 (b)). This mainly lies in the fact that KU is capable of amplifying the residual errors and making fault detection more sensitive. As shown in Fig.3 (b), the control limit of SPE_{KU} is learned from the training data, whose significant level is 0.05. For SPE, Type II error is equal to

4/20=20% and Type I error is equal to 95/143=66.4%. However, for SPE_{KU}, Type II error is equal to 0/20=0% and Type I error is equal to 3/143=2.1%. Therefore, it is obvious that SPE_{KU} achieved better performance than SPE in terms of Type II and Type I errors. To fully compare with other typical fault detection methods, PCA-based and ICA-based methods are also implemented. PCA-based and ICA-based SPE achieved similar performance with CCA counterpart, but still performed worse than CCA-based SPE_{KU} (Fig. 3 (c) and Fig. 3 (d)) in terms of Type II and Type I errors.

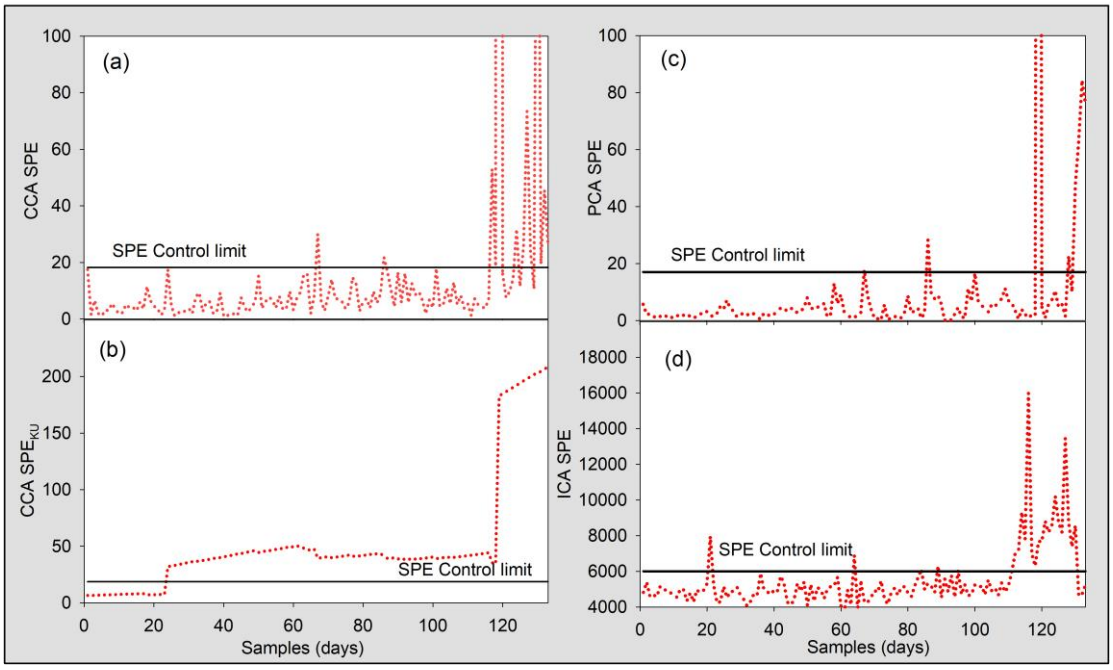

Fig. 3 SPE-based Fault detection with PCA, ICA and CCA

3.4 Fault identification

Traditionally, contribution plot based fault identification methods usually result in smearing effect and then leading to false identification. To deal with this problem, KU is firstly used to extract features for each variable as shown in Fig.4. To further capture the variation features, the variation rate, KA_i, is designed to assess the true occurrence time. Based on Eq. (8), the degree of variations for each variable can be derived. As profiled in Fig. 4, the variables, $[T, BOD_5, TP, COD, SNO]$, exhibit significant variations during different time domain, but others are not. It is import to notice that the sludge bulking occurs at the 70th day (20th day in the testing dataset)

and it is identified at the 73th day (23th day in the testing dataset). During this period, the obvious variations can be only seen from T and BOD_5. Due to the time delay among variables, it is reasonable to assume that the occurrence of abnormal events for the first time could be the source of a fault. Therefore, the sequences of variables in the original data set are reorganized as the first column of Table I. Since the filamentous sludge bulking is typically indicated by SVI, SVI serves as the target variable and tabulates as Table 1 (Row 10, Column 10). The reason why the proposed framework re-organizes variable sequence herein is that the core of MVGC is time series analysis favoring temporal features and re-organization of variables is able to facilitate the graphical representation.

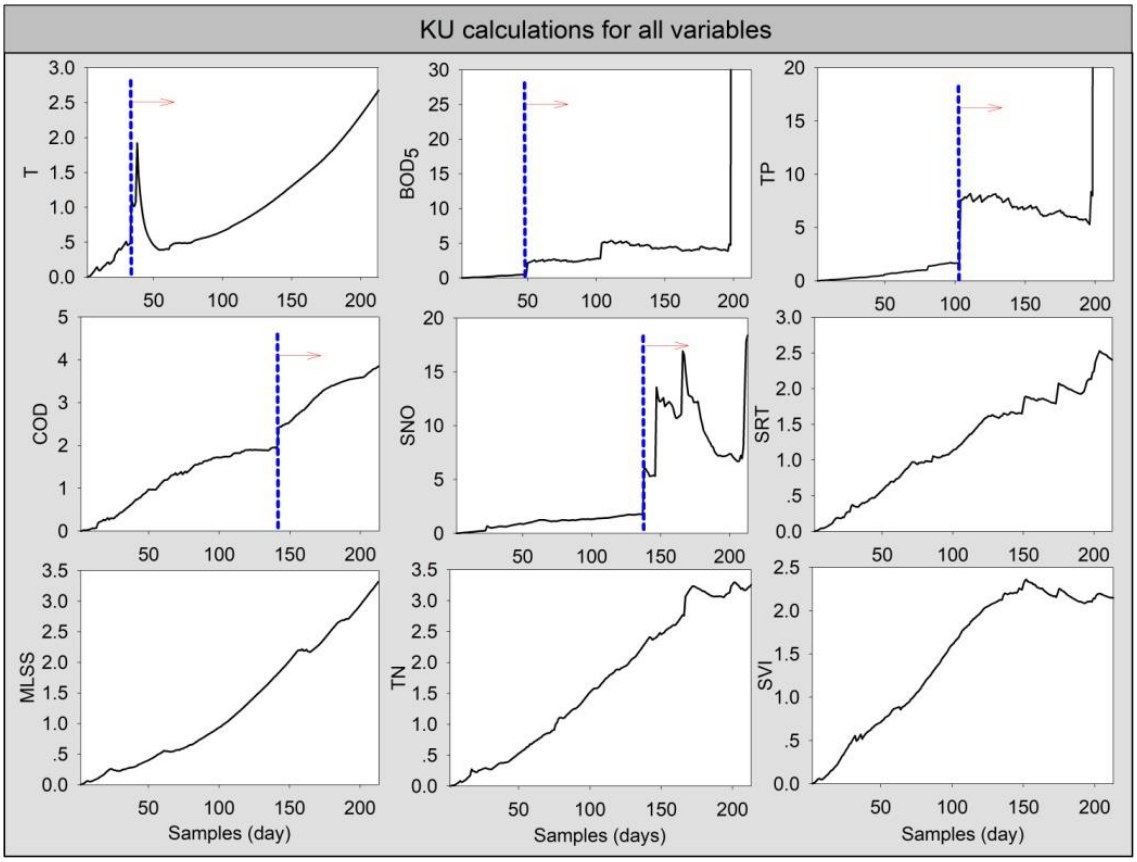

Fig. 4 Feature extraction for each raw variable by KU

The refined features by KU are then fed to MVGC for causality analysis. The causal results as tabulated in Table 1 show that the highlighted red cells suggest the maximum causal effect of column variables among variables. Fig. 5 further shows the

first-highest causal relationship among variables, i.e., COD, SVI and MLSS. Moreover, the causality network is built as Fig. 5 based on the cause-effect correlation of Table 1. During the network construction, since $F_{SRT \to MLSS} > F_{MLSS \to SRT}$ (Table 1), direction $F_{SRT \to MLSS}$ is selected. This can be explained by the fact that longer SRT is indeed able to result in higher MLSS. In the mean time, $F_{T \to SVI} > F_{SVI \to T}$ (Table 1), direction $F_{T \to SVI}$ is selected. The temperature variation mainly comes from influence of external environment, rather than the treatment processes itself. Thus, it is reasonable to explain that the varied temperature *T* will lead to the variation of SVI by affecting the bacteria behaviors. The results in Fig. 5 suggest that, due to acting as the most sources for other variables, *T* has the highest probability to be the cause of the occurrence of a fault and SVI is the final target variable. It deserved to notice from Fig.5 that both solid lines that generated from T are able to converge into SVI. One is T->SVI. The other is T->COD->TN->SRT->MLSS->SVI. Both represent the relative highest probability of the fault propagation. Therefore, the developed algorithm for fault amplification can be efficiently used to indicate the fault propagation path in a graphical way.

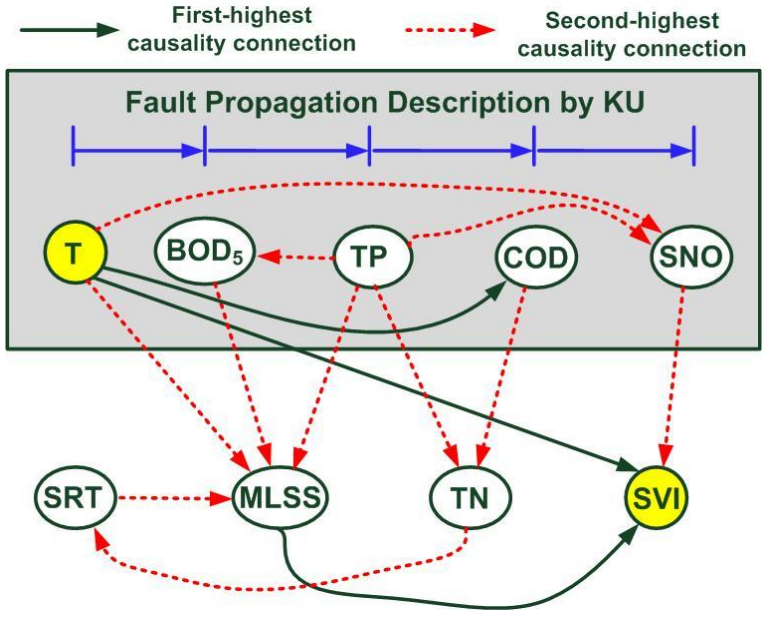

Fig. 5 Fault propagation route

3.5 Fault prognosis and RUL prediction

To implement the RUL prediction, ARMA is used for multi-step-ahead prediction

of SVI firstly over a long term once the incipient fault is declared by the SPE_{KU} at the 23^{rd} day (during the testing dataset). The data are treated by the first-order differencing. Then, the orders for AR term and MA term are selected for 3 and 1, respectively by analyzing the ACF (Auto-correlation Function) and PCF (Partial correlation Function) (More details can see the Supplementary Information). 36 steps ahead predictions are derived in this case study. Among them, 9-step,18-step,27-step and 36-step ahead predictions are shown in Fig. 6, suggesting that all the prediction results are acceptable, even though the prediction performance is accompanied by somehow deterioration as more steps ahead prediction is performed (Table 2). The deterioration is mainly due to lack of necessary information to compensate the prediction deviation as prediction horizon moves ahead. It is important to notice that the deterioration is not that obvious between the 23^{rd} day and 43^{rd} day. On the contrary, the deterioration of multi-step-ahead prediction become more obvious after the 55^{th} day. This can be partly explained that an ARMA model is linear model and more suitable for a fairly stationary process (0-43^{rd} day), whereas performs worse in the non-stationary process (after the 43^{rd} day). After the incipient fault declaration, the fault costs 32 days to reach the control limit, 200 mg/L, for the first time. That is, RUL is equal to 32 in this case study. It is important to notice in Fig. 6 that the uncertainty level of 36-day-ahead prediction using an ARMA model can be profiled as an envelope. Even though uncertainties from the former algorithm chain (CCA-SPE-KU-MVGC-ARMA) cannot be described by each step, all of them can be ultimately reflected upon the uncertainty level of the ARMA-based predictions. If conserved decision-making is necessary, 36-day-ahead upper limit will be preferred to decide the RUL. RUL is equal to 26, which is 6-day-ahead over the scenario depending on the mean values based decision-making.

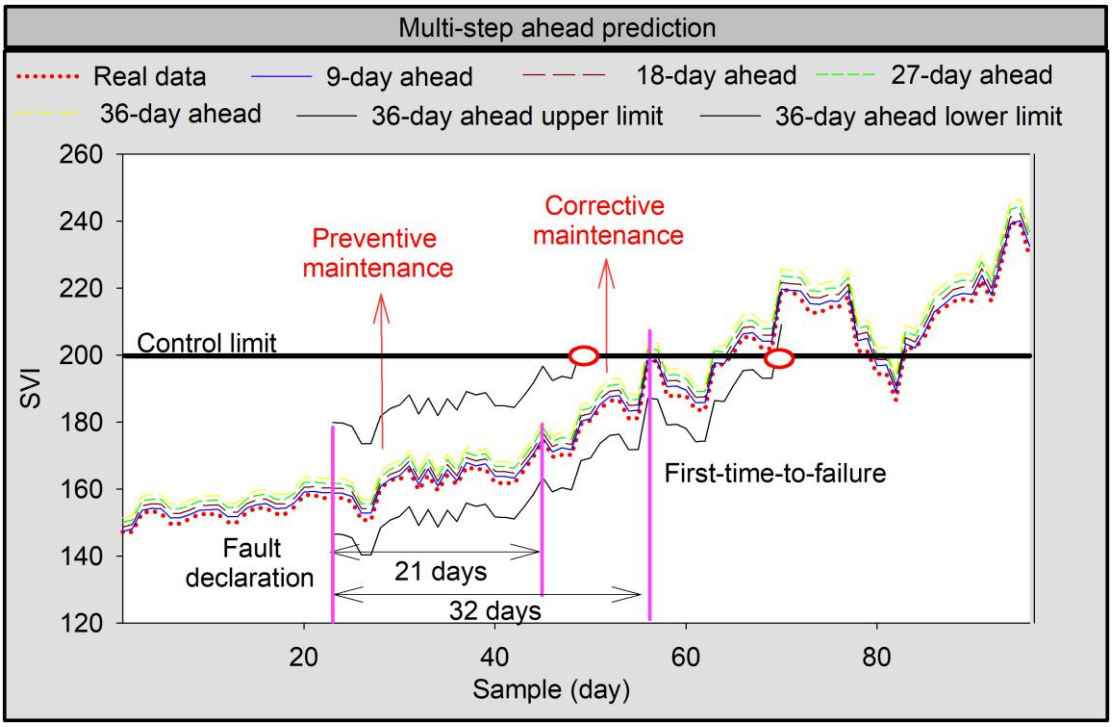

Fig. 6 Multi-step prediction on the basis of an ARMA model

Table 2 RMSE and r_c of multi-step prediction using a ARMA model

Index	9-day-ahead	18-day-ahead	27-day-ahead	36-day-ahead
RMSE	1.63	3.19	4.83	6.5
r_c	0.983	0.975	0.967	0.959

3.6 Maintenance strategy

By aforementioned analysis, the sludge bulking stems from abnormal temperature variations. In wastewater treatment system, seasonal variations always induce temperature oscillations, therefore imposing negative influence on the metabolic activities for the microbial population and the gas-transfer rates as well as the settling characteristics of activated sludge. Typically, 25-35 ℃ is considered as the optimum temperatures for common bacteria. Particularly, when the temperature dropped to around 5 ℃, the autotrophic nitrifying bacteria will de-function. Once the control limit of SPE_{KU} is reached, preventive maintenance is triggered. To deal with this problem, preventive maintenance actions are implemented with the aid of Table S1 (Supplementary Information). The day that the SPE_{KU} is reached is 23rd and SVI is

equal to 157.3 mg/L. CCL_{limit} can be derived as 178.3 mg/L by Eq. (21). Therefore, 21 days are kept for preventive maintenance, the remaining 11 days are left for corrective maintenance. To minimize the negative effect of temperatures during preventive maintenance stage, adjustment of operational parameters is necessary, including SRT, C/N ratio, pH, TN and SNO. By analyzing Fig. 5, SRT, BOD_5 and TP can have direct effect on SVI through MLSS. In a wastewater plant, SRT is the most convenient factor among them to adjust. Once the preventive maintenance strategy does not work well and the CCL_{limit} is attained, corrective maintenance has to be triggered. During this stage, we have to further add coagulants or $FeSO_4$ to kill filamentous bacteria. However, in case that SVI crosses over 200 mg/L, we have to shut down the wastewater plant to avoid polluted wastewater discharge into river. Additionally, it is worthwhile to notice that, by defining preventive and corrective maintenance for sludge bulking control, a guideline can be formed and the operators could achieve better control performance with lower operational cost, rather than operating in an ad-hoc way.

3.7 Discussion: implications, implementation and future research

The present work proposes a condition-based maintenance framework. In this novel hybrid framework, fault detection, location, propagation identification, remaining useful life (RUL) prediction and maintenance are performed for sludge bulking control. This is the first attempt to propose a framework for sludge bulking management systematically, providing water utilities with a tool for sludge bulking control. The results showed that this framework can be successfully applied to filamentous sludge bulking management. To facilitate discussions, a flowchart that briefly the calculation process is shown as Fig. 7.

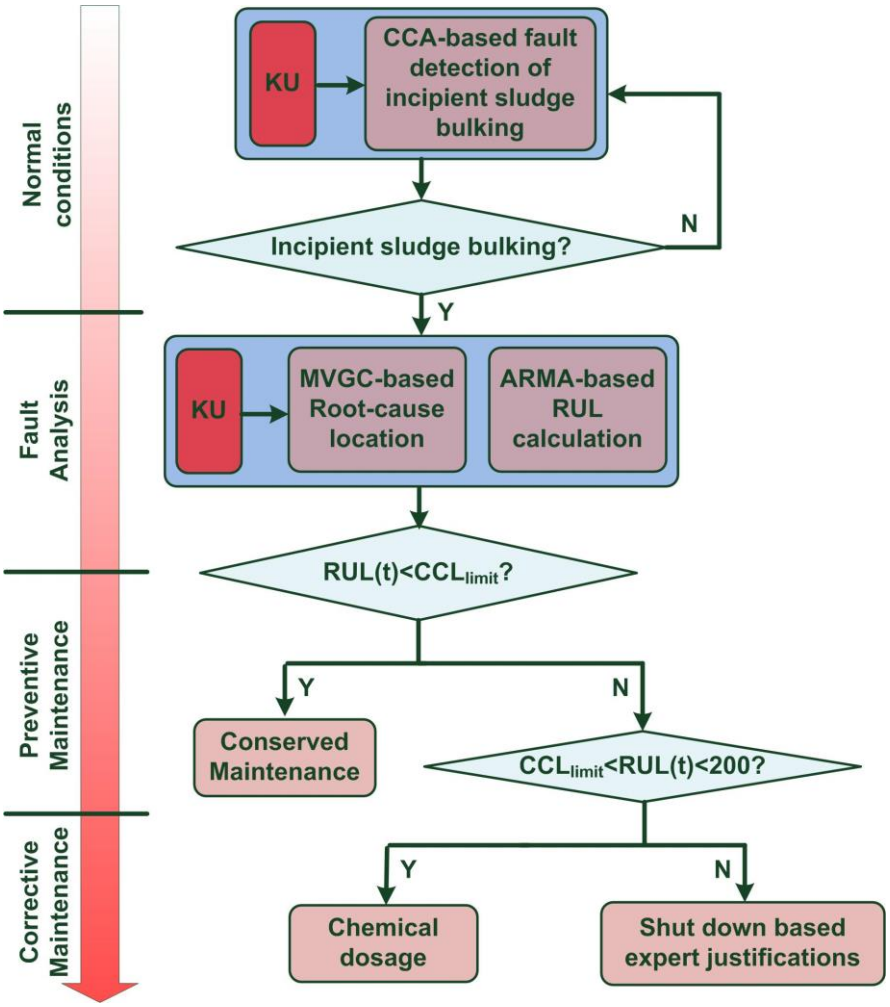

Fig. 7 The flowchart of proposed framework

In this work, even though PCA, ICA and PLS could perform better than CCA or maybe not, it is still the first attempt to use statistical method to serve as a pre-alarm system rather than just act as a fault detection component. Also, MVGC, ARMA and KU can be substituted by their similar algorithms if necessary. In fact, the motive behind this paper is to overcome the limitations of individual methods and strengthen global system collaboration by coordinating CCA, MVGC, ARMA, KU and Expert knowledge from a systematic point of view. Another issue in this work is the uncertainty analysis of hyper-parameters, such as the order of ARMA model, the number of latent variables for CCA, the percentage to separate RUL for preventive and corrective maintenance, and so on. One of potentials is resorting to build a meta-analysis model upon the system, which is able to use heuristic methods, such as Artificial Bee Colony, Cuckkoo search, Firefly algorithm and so on (Cheng, Chou, &

Cao, 2017), to optimize these hyper-parameters automatically, rather than depend on empirical setting. In addition, since the algorithms, i.e., CCA-SPE-KU-MVGC-ARMA-Expert knowledge table, is serially connected with each other in the proposed framework, a slight fault in the former component could lead to the latter system failure. Even if these issues cannot be fully solved, the maintenance and operations are indeed alleviated significantly by involvement of operators in the fault detection, location and prognosis components. Moreover, to assess these uncertainties, sensitivity analysis is one of alternatives able to gain essential insights on algorithm behavior, on its structure and on its response to changes in the algorithm inputs (Feng, et al., 2019). Local sensitivity analysis methods (such as generalized tornado diagrams, Spiderplots, Differentiation-based methods, and so on) and global sensitivity analysis methods (such as Monte-Carlo-simulation, Gaussian processes model, Bayesian Networks, and so on) have been developed, giving rise to the chain behaviors exploration (Borgonovo & Plischke, 2016; Pianosi, et al., 2016). Another solution is to take the algorithm chain as a serial system for reliability analysis (Feng, et al., 2019; B. Liu, Yeh, Xie, & Kuo, 2017). It is also important to notice that the condition-based maintenance is a partially automatic rather than a fully automatic system. This represents that human maintenance behavior is also necessary and formulates a Human-Cyber-Physical Systems (HCPS) for optimization (He, Chan, Qiao, & Guizani, 2018).

In this article, KU is able to improve CCA and MVGC to make them more sensitive to detect and locate the root of the fault. KU is sensitive to impulsive faults, especially incipient faults, but are less effective for performance degradation assessment because filter-based kurtosis value decreases gradually as fault severity grows. However, other indicators, such as the root mean square (RMS), have less sensitivity to impulse faults, but can reflect the growth of fault severity. Coordination of KU and other indicators to improve the effectiveness can be studied in future. In our case studies, *RMSE* and correlation coefficient (r_c) are used to assess the prediction performance of an ARMA model. To clarify and enhance comparison of a model prediction performance, mean

absolute error (MAE), mean absolute relative error (MARE), Bias statistical parameters, Akaike Information Criterion (AIC), mean squared error (MSE), Bayesian Information Criterion (BIC) or Schwarz Bayesian Criterion (SBC) can be also served as performance indicators (Bonakdari, Zaji, Shamshirband, Hashim, & Petkovic, 2015; Can, Tosunoglu, Lu, & Kahya, 2012; Isa Ebtehaj, Bonakdari, Moradi, Gharabaghi, & Khozani, 2018; Shaghaghi, Bonakdari, Gholami, & Ebtehaj, 2017; Yurekli, Kurunc, & Ozturk, 2005). The prediction model used in MVGC is an ARMA model, which is limited in capturing linear relationship among variables. The next step will extend MVGC to nonlinear MVGC or enhance transfer entropy based causality analysis. In terms of field implementation, this methodology has been designed as simple as possible, thus should be implementable in most of the commercially available PLC systems.

4 Conclusions

A novel condition-based maintenance framework, consisting of fault detection, location, identification, RUL prediction and maintenance, was proposed and applied to an oxidation process for filamentous sludge bulking management. In this framework, CCA with Kurtosis indicator was indeed able to capture the sludge bulking features as earlier as possible with Type I error and Type II error being 2.1% and 0%, respectively. Sequentially, MVGC was feasible to diagnose the root cause of the fault and showed the propagation pathways of the fault in the system graphically. 32-steps-ahead predictions were derived by a virtual measurement (an ARMA model) and assessed in terms of *RMSE* (6.5) and r_c (0.959). Given the prediction outcome of the virtual sensor, an associated maintenance strategy was suggested to intervene the filamentous sludge bulking. Compared with the existing methods, the proposed framework exhibits a distinct advantage to treat the maintenance a systematic point of and provide a guideline for filamentous sludge bulking management. Last but not least, we envision reasonably that correctly locating the root-cause of sludge bulking and timely recognizing the fault evolutions are able to avoid under-intervention or

over-intervention bulking management, thus saving more work force and chemical dosage costs. Without loss of generality, the proposed framework is applicable to manage other degradation processes, such as material corrosion, sensor drifting errors, and so on. However, the coordination of preventive and corrective maintenance is not globally optimized. In the future research, we will investigate on integrating maintenance with evolutionary algorithms to optimally assign preventive and corrective tasks.

Acknowledgement

This work was supported by the National Natural Science Foundation of China (61873096, 61673181), the Science and Technology Program of Guangzhou, China (201804010256).

References

Allison AEF, Dickson ME, Fisher KT, & Thrush SF. Dilemmas of modelling and decision-making in environmental research. Environmental Modelling & Software 2018;99:147-155.

Asendorf N, & Nadakuditi RR. Improved Detection of Correlated Signals in Low-Rank-Plus-Noise Type Data Sets Using Informative Canonical Correlation Analysis (ICCA). IEEE Transactions on Information Theory 2017;63:3451-3467.

Bonakdari H, Moeeni H, Ebtehaj I, Zeynoddin M, Mahoammadian A, & Gharabaghi B. New insights into soil temperature time series modeling: linear or nonlinear? Theoretical and Applied Climatology 2019;135:1157-1177.

Bonakdari H, Zaji A, Binns A, & Gharabaghi B. Integrated Markov chains and uncertainty analysis techniques to more accurately forecast floods using satellite signals. Journal of Hydrology 2019;572.

Bonakdari H, Zaji AH, Shamshirband S, Hashim R, & Petkovic D. Sensitivity analysis of the discharge coefficient of a modified triangular side weir by adaptive neuro-fuzzy methodology. Measurement 2015;73:74-81.

Borgonovo E, & Plischke E. Sensitivity analysis: A review of recent advances. European Journal of Operational Research 2016;248:869-887.

Cai B, Liu H, & Xie M. A real-time fault diagnosis methodology of complex systems using object-oriented Bayesian networks. Mechanical Systems and Signal Processing 2016;80.

Cai B, Zhao Y, Liu H, & Xie M. A Data-Driven Fault Diagnosis Methodology in Three-Phase Inverters for PMSM Drive Systems. IEEE Transactions on Power Electronics 2017;32:5590-5600.

Can I, Tosunoglu F, Lu, & Kahya E. Daily streamflow modelling using autoregressive moving average and artificial neural networks models: Case study of Çoruh basin, Turkey. Water and Environment Journal 2012;26.

673 Chen J, Ganigue R, Liu Y, & Yuan Z. Real-Time Multistep Prediction of Sewer Flow for Online Chemical
674 Dosing Control. Journal of Environmental Engineering 2014;140.
675 Chen Z, Ding SX, Zhang K, Li Z, & Hu Z. Canonical correlation analysis-based fault detection methods
676 with application to alumina evaporation process. Control Engineering Practice 2016;46:51-58.
677 Chen Z, Zhang K, Ding SX, Shardt YAW, & Hu Z. Improved canonical correlation analysis-based fault
678 detection methods for industrial processes. Journal of Process Control 2016;41:26-34.
679 Cheng M-Y, Chou J-S, & Cao M-T. Nature-inspired metaheuristic multivariate adaptive regression
680 splines for predicting refrigeration system performance. Soft Computing 2017;21:477-489.
681 de la Rosa JJG, Agüera Pérez A, Palomares Salas JC, & Sierra Fernández JM. A novel measurement
682 method for transient detection based in wavelets entropy and the spectral kurtosis: An
683 application to vibrations and acoustic emission signals from termite activity. Measurement
684 2015;68:58-69.
685 Ding SX. Canonical Variate Analysis Based Process Monitoring and Fault Diagnosis. Data-driven Design
686 of Fault Diagnosis and Fault-tolerant Control Systems. London: Springer London; 2014. p.
687 117-131.
688 Ebtehaj I, Bonakdari H, & Gharabaghi B. A reliable linear method for modeling lake level fluctuations.
689 Journal of Hydrology 2019;570.
690 Ebtehaj I, Bonakdari H, Moradi F, Gharabaghi B, & Khozani ZS. An integrated framework of Extreme
691 Learning Machines for predicting scour at pile groups in clear water condition. Coastal
692 Engineering 2018;135:1-15.
693 Ebtehaj I, Bonakdari H, Zeynoddin M, Gharabaghi B, & Azari A. Evaluation of preprocessing techniques
694 for improving the accuracy of stochastic rainfall forecast models. International Journal of
695 Environmental Science and Technology 2019.
696 Fan N, Wang R, Qi R, Gao Y, Rossetti S, Tandoi V, & Yang M. Control strategy for filamentous sludge
697 bulking: Bench-scale test and full-scale application. Chemosphere 2018;210:709-716.
698 Feng Q, Zhao X, Fan D, Cai B, Liu Y, & Ren Y. Resilience design method based on meta-structure: A case
699 study of offshore wind farm. Reliability Engineering & System Safety 2019;186:232-244.
700 Ge Z. Process Data Analytics via Probabilistic Latent Variable Models: A Tutorial Review. Industrial &
701 Engineering Chemistry Research 2018;57:12646-12661.
702 Guo J, Zhang L, Chen W, Ma F, Liu H, & Tian Y. The regulation and control strategies of a sequencing
703 batch reactor for simultaneous nitrification and denitrification at different temperatures.
704 Bioresource Technology 2013;133:59-67.
705 Hartley KJ. Controlling sludge settleability in the oxidation ditch process. Water Research
706 2008;42:1459-1466.
707 He D, Chan S, Qiao Y, & Guizani N. Imminent Communication Security for Smart Communities. Ieee
708 Communications Magazine 2018;56:99-103.
709 Jiang Q, Yan X, & Huang B. Performance-Driven Distributed PCA Process Monitoring Based on
710 Fault-Relevant Variable Selection and Bayesian Inference. IEEE Transactions on Industrial
711 Electronics 2016;63:377-386.
712 Joanes D, & Gill CA. Comparing Measures of Sample Skewness and Kurtosis. Journal of the Royal
713 Statistical Society: Series D (The Statistician) 1998;47:183-189.
714 Kenway SJ, Binks A, Lane J, Lant PA, Lam KL, & Simms A. A systemic framework and analysis of urban
715 water energy. Environmental Modelling & Software 2015;73:272-285.
716 Lee J-M, Qin SJ, & Lee I-B. Fault detection and diagnosis based on modified independent component

717 analysis. AIChE Journal 2006;52:3501-3514.
718 Lee J, Kang B, & Kang S-H. Integrating independent component analysis and local outlier factor for
719 plant-wide process monitoring. Journal of Process Control 2011;21:1011-1021.
720 Liu B, Liang Z, Parlikad AK, Xie M, & Kuo W. Condition-based maintenance for systems with aging and
721 cumulative damage based on proportional hazards model. Reliability Engineering & System
722 Safety 2017;168:200-209.
723 Liu B, Wu S, Xie M, & Kuo W. A condition-based maintenance policy for degrading systems with age-
724 and state-dependent operating cost. European Journal of Operational Research
725 2017;263:879-887.
726 Liu B, Yeh R, Xie M, & Kuo W. Maintenance Scheduling for Multicomponent Systems with Hidden
727 Failures. IEEE Transactions on Reliability 2017;66:1280-1292.
728 Liu H, Yang C, Huang M, Wang D, & Yoo C. Modeling of Subway Indoor Air Quality Using Gaussian
729 Process Regression. Journal of Hazardous Materials 2018;359.
730 Liu Y, Liu B, Zhao X, & Xie M. A Mixture of Variational Canonical Correlation Analysis for Nonlinear and
731 Quality-Relevant Process Monitoring. IEEE Transactions on Industrial Electronics
732 2018;65:6478-6486.
733 Liu Y, Liu B, Zhao X, & Xie M. Development of RVM-Based Multiple-Output Soft Sensors With Serial
734 and Parallel Stacking Strategies. IEEE Transactions on Control Systems Technology
735 2019;27:2727-2734.
736 Martins AMP, Pagilla K, Heijnen JJ, & van Loosdrecht MCM. Filamentous bulking sludge—a critical
737 review. Water Research 2004;38:793-817.
738 Merello P, García-Diego F-J, & Zarzo M. Diagnosis of abnormal patterns in multivariate microclimate
739 monitoring: A case study of an open-air archaeological site in Pompeii (Italy). Science of The
740 Total Environment 2014;488-489:14-25.
741 Moeeni H, & Bonakdari H. Forecasting monthly inflow with extreme seasonal variation using the
742 hybrid SARIMA-ANN model. Stochastic Environmental Research and Risk Assessment
743 2017;31:1997-2010.
744 Moeeni H, & Bonakdari H. Impact of Normalization and Input on ARMAX-ANN Model Performance in
745 Suspended Sediment Load Prediction. Water Resources Management 2018;32:845-863.
746 Montserrat A, Bosch L, Kiser MA, Poch M, & Corominas L. Using data from monitoring combined
747 sewer overflows to assess, improve, and maintain combined sewer systems. Science of The
748 Total Environment 2015;505:1053-1061.
749 Narayana Moorthy NSH, Martins SA, Sousa SF, Ramos MJ, & Fernandes PA. Classification study of
750 solvation free energies of organic molecules using machine learning techniques. RSC
751 Advances 2014;4:61624-61630.
752 Ng WJ, Ong SL, & Hossain F. An algorithmic approach for system-specific modelling of activated sludge
753 bulking in an SBR. Environmental Modelling & Software 2000;15:199-210.
754 Olsson G. ICA and me – A subjective review. Water Research 2012;46:1585-1624.
755 Ovez S OD. Microbial Ecology of Bulking and Foaming Activated Sludge Treating Tannery Wastewater. J
756 Env Sci Health, Part A 2007;40:409-422.
757 Pianosi F, Beven K, Freer J, Hall JW, Rougier J, Stephenson DB, & Wagener T. Sensitivity analysis of
758 environmental models: A systematic review with practical workflow. Environmental
759 Modelling & Software 2016;79:214-232.
760 Rensink JH. New Approach to Preventing Bulking Sludge. Journal (Water Pollution Control Federation)

761 1974;46:1888-1894.
762 Rossetti S, Tomei MC, Nielsen PH, & Tandoi V. "Microthrix parvicella", a filamentous bacterium causing
763 bulking and foaming in activated sludge systems: a review of current knowledge. Fems
764 Microbiol Rev 2005;29:49-64.
765 Sarrigiannis YZSABH-LWPG. A Parametric Method to Measure Time-Varying Linear and Nonlinear
766 Causality With Applications to EEG Data. IEEE Transactions on Biomedical Engineering
767 2013;8:3141 - 3148.
768 Seth AK. A MATLAB toolbox for Granger causal connectivity analysis. Journal of Neuroscience Methods
769 2010;186:262-273.
770 Shaghaghi S, Bonakdari H, Gholami A, & Ebtehaj I. Comparative analysis of GMDH neural network
771 based on genetic algorithm and particle swarm optimization in stable channel design. Applied
772 Mathematics and Computation 2017;313.
773 Vicente R, Wibral M, Lindner M, & Pipa G. Transfer entropy—a model-free measure of effective
774 connectivity for the neurosciences. Journal of Computational Neuroscience 2011;30:45-67.
775 Vitale R, de Noord OE, & Ferrer A. Pseudo-sample based contribution plots: innovative tools for fault
776 diagnosis in kernel-based batch process monitoring. Chemometrics and Intelligent Laboratory
777 Systems 2015;149:40-52.
778 Wang J, Yang F, Chen T, & Shah SL. An Overview of Industrial Alarm Systems: Main Causes for Alarm
779 Overloading, Research Status, and Open Problems. IEEE Transactions on Automation Science
780 and Engineering 2016;13:1045-1061.
781 Yurekli K, Kurunc A, & Ozturk F. Application of linear stochastic models to monthly flow data of Kelkit
782 Stream. Ecological Modelling 2005;183:67-75.
783 Zeynoddin M, Bonakdari H, Azari A, Ebtehaj I, Gharabaghi B, & Riahi Madavar H. Novel hybrid linear
784 stochastic with non-linear extreme learning machine methods for forecasting monthly rainfall
785 a tropical climate. Journal of Environmental Management 2018;222:190-206.
786 Zeynoddin M, Bonakdari H, Ebtehaj I, Esmaeilbeiki F, Gharabaghi B, & Zarehaghi D. A Reliable Linear
787 Stochastic Daily Soil Temperature Forecast Model. Soil and Tillage Research 2018;189.
788 Zhu J, Ge Z, & Song Z. Distributed Parallel PCA for Modeling and Monitoring of Large-Scale Plant-Wide
789 Processes With Big Data. IEEE Transactions on Industrial Informatics 2017;13:1877-1885.
790
791